On-Chip Cell Lysis by Antibacterial Non-Leaching Reusable Quaternary Ammonium Monolithic Column†

Mohamed Aly Saad Aly,[a] **Mario Gauthier,**[b] **and John Yeow**[*a]

ABSTRACT: Reusable antibacterial non-leaching monolithic columns polymerized in microfluidic channels designed for on-chip cell lysis applications were obtained by the photoinitiated free radical copolymerization of diallyldimethylammonium chloride (DADMAC) and ethylene glycol diacrylate (EGDA) in the presence of a porogenic solvent. The microfluidic channels were fabricated in cross-linked poly(methyl methacrylate) (X-PMMA) substrates by laser micromachining. The monolithic columns have the ability to inhibit the growth of, kill and efficiently lyse gram-positive Micrococcus luteus (Schroeter) (ATCC 4698) and Kocuria rosea (ATCC 186), and gram-negative bacteria Pseudomonas putida (ATCC 12633) and Escherichia coli (ATCC 35218) by mechanically shearing the bacterial membrane when forcing the cells to pass through the narrow pores of the monolithic column, and simultaneously disintegrating the cell membrane by physical contact with the antibacterial surface of the column. Cell lysis was confirmed by off-chip PCR without the need for further purification. The influence of the cross-linking monomer on bacterial growth inhibition, leaching, lysis efficiency of the monolithic column and its mechanical stability within the microfluidic channel were investigated and analyzed for three different cross-linking monomers: ethylene glycol dimethacrylate (EGDA), ethylene glycol dimethacrylate (EGDMA) and 1,6-hexanediol dimethacrylate (1,6-HDDMA). Furthermore, the bonding efficiency of two X-PMMA substrates with different cross-linking levels was studied. The monolithic columns were shown to be stable, non-leaching, and reusable for over 30 lysis cycles without significant performance degradation or DNA carryover when they were back-flushed between lysis cycles.

Acknowledgements

We would like to express our gratitude to Grand Challenges Canada and Bigtec Labs for their financial support. We also thank Prof. Michael Palmer, Mr. Mohamed Salah, and Mr. Eric K. Brefo-Mensah, from the Department of Chemistry at the University of Waterloo, for providing access to their lab facilities and their guidance on some of the biological concepts.

Keywords Porous Polymeric Monolith; Cell Lysis; Antibacterial; Quaternary Ammonium; Reusable; Growth inhibition; Non-Leaching

---

[a] Department of Systems Design Engineering, University of Waterloo, 200 University Ave West, Waterloo, Ontario, Canada N2L 3G1. E-mail: jyeow@uwaterloo.ca; Fax: +1 519 746-4791; Tel: +1 519 888-4567 Ext. 32152

[b] Department of Chemistry, University of Waterloo

† **Electronic supplementary material** The online version of this article (DOI: 10.1007/s10544-015-0025-z, 2016) contains supplementary material, which is available to authorized users.

The final publication is available at Springer via http://dx.doi.org/10.1007/s10544-015-0025-z

1. Introduction

Antimicrobial polymers have the ability to constrain the growth and eventually kill microorganisms such as bacteria, fungi, and sometimes viruses. An antimicrobial surface is typically formed by a polymer killing cells upon contact. At the beginning of this century, surfaces that killed bacteria upon contact were introduced and this phenomenon was termed ‘contact killing’ (Tiller et al. 2001). Development is progressing to engineer these polymers in order to copy the characteristic of natural host defense peptides (HDPs) utilized by the immune system in living life forms to fight microscopic organisms. That rising family of antimicrobial polymers, called `synthetic mimics of antimicrobial peptides' (SMAMPs), is formed to emulate the principle elements of HDPs: cationic charge and amphiphilic character, which prompt the imbuing and afterward the breakdown of the bacterial membrane (Lienkamp et al. 2008).

Polymers containing quaternary ammonium compounds (QACs) are another class of antibacterial polymers widely used as biocides and disinfectants. In this class of materials no antibacterial units are leaching, providing permanent protection against bacterial reproduction (Dizman et al. 2006). The positive surface charges intrinsically inherited from the quaternary ammonium-functionalized surfaces strongly adhere to negatively charged bacterial membranes, which inhibits bacterial growth, kills and eventually lyses rod-shaped bacteria by penetrating their membrane and causing the outflow of intracellular material (Harkes et al. 1992). The polymers have been covalently attached onto various materials by numerous techniques such as ‘grafting to’ (Tiller et al. 2001), ‘grafting from’ (Biesalski and Ruhe 1999), atom transfer radical polymerization (ATRP) (Lee et al. 2004), surface-initiated ATRP (Murata et al. 2007) on glass, UV-induced surface graft polymerization on polymer and paper (Cen et al. 2004), and ‘grafting from’ mediated radical polymerization on metals (Ignatova et al. 2004).

Diallyldimethylammonium chloride (DADMAC) is a quaternary ammonium and positively charged monomer potentially useful for that purpose. It possesses high water solubility, alkenyl double bond in its molecular structure, and can form hydrophilic homopolymers and copolymers by various polymerization reactions. Poly(diallyldimethylammonium chloride), polyDADMAC, is a polymer with a permanent high cationic charge density (independently of pH), is non-bioaccumulable, non-biodegradable, and adsorbs onto negatively charged surfaces such as bacterial membranes (Thome et al. 2003). It was reported that polyDADMAC can inhibit microbial growth (Koslow 2007). It was reported that polyDADMAC possesses strong bacterial adhesion, moreover it has high contact killing activity against waterborne pathogens (Raoultella terrigena, Escherichia coli, and Brevundimonas diminuta) (Mei et al. 2008). Bacterial barrier dressings treated with polyDADMAC was developed to prevent wound infection that absorbed wound exudate while not releasing toxic materials into the wound (Mikhaylova et al. 2011). These dressings were capable of disrupting bacterial membranes, resulting in cell lysis and death.

Antibacterial films were developed by blending konjac glucomannan (KGM) and polyDADMAC in aqueous media (Lu et al. 2008). It was concluded that the films efficiently inhibited the growth and lysed gram-positive bacteria (Bacillus subtilis and Staphylococcus aureus), and was less efficient toward gram-negative bacteria (Escherichia coli and Pseudomonas aeruginosa). An ultrathin (1-2 nm) antibacterial polyDADMAC film was added on polymer surfaces by the ‘grafting to’ technique via radical polymerization (Thome et al. 2003). These films reduced the accumulation of bacterial cells including Micrococcus luteus (gram-positive) and Escherichia coli (gram-negative) by a factor of 10^6-10^7.

Porous polymeric monoliths (PPMs) were introduced over the past ten years and are mainly used in liquid chromatography and for deoxyribonucleic acid (DNA) isolation. PPMs are usually prepared within capillaries and microfluidic channels by free radical polymerization of a mixture that includes a functional monomer, a cross-linking monomer, a free-radical initiator, and porogenic solvents. The PPMs were used as of late for cell lysis inside of microchips (Mahalanabis et al. 2009; Sauer-Budge et al. 2009), in which the bacterial cells were lysed by mechanical shearing of the cell walls by stream into a PPM polymerized inside a microfluidic channel assisted with chemical lysis.

Multi-walled carbon nanotubes were impregnated in the PPMs and asserted to enrich the lysis efficiency, albeit with chemical and enzymatic pretreatments of the bacterial cells (Bhattacharyya et al. 2008).

We recently lysed gram-negative and gram-positive bacteria by flowing through an antibacterial PPM polymerized into an X-PMMA microfluidic channel without previous chemical or enzymatic treatment. In that work, the PPM was synthesized with a functional monomer belonging to the 'SMAMPs' class of antibacterial polymers (Aly Saad Aly et al. 2013). To demonstrate that cells were lysed via a dual mechanism, the active (functional) monomer, N-(*tert*-butyloxycarbonyl)aminoethyl methacrylate (Boc-AEMA) was first used in its Boc-protected form to demonstrate mechanical shearing lysis alone. Once the protecting group was removed the PPM became antibacterial, leading to improved performance. Both lysis mechanisms were thus validated (Aly Saad Aly et al. 2013). Furthermore, we improved the lysis efficiency of the PPMs by tuning their hydrophobic-hydrophilic balance and determining the optimal flow rate, at which the bacterial cell walls were sufficiently mechanically sheared through the porous medium of the column to disrupt the cell membrane by physical contact with the antibacterial polymeric biocide covering the pore surface (Aly Saad Aly et al. 2014). In the current investigation, we developed an antibacterial PPM from a functional monomer that contains QAC, which is intrinsically cationic and antibacterial. We also studied the effect of the cross-linking monomer on bacterial growth inhibition, lysis efficiency and the mechanical stability of the PPM column within the microfluidic channel, using three different cross-linking monomers and different cross-linker contents in the X-PMMA substrate. Moreover, the bonding efficiency between the different components was examined for varying cross-linking levels of the X-PMMA substrate. Furthermore, the reusability of the QACs-PPM was investigated and compared with the previously developed SMAMP-PPMs.

2. Experimental

2.1 Materials

Methyl methacrylate (MMA, 99 %), ethylene glycol dimethacrylate (EGDMA, 98 %), and 1,6-hexanediol dimethacrylate (1,6-HDDMA, ≥90 %) were all purchased from Sigma-Aldrich (Oakville, ON Canada), and filtered over alumina to remove inhibitors. Diallyldimethylammonium chloride (DADMAC, 65 wt% in H_2O), 2,2-dimethoxy-2-phenylacetophenone (DMPAP, 99 %), ethylene glycol diacrylate (EGDA, 90 %), methanol (≥99.9 % Chromasolv), potassium bromide (ACS reagent, 99.0 % , KBr), and fumed silica (powder, 0.2-0.3 µm average particle size) were purchased from Sigma-Aldrich and were used without further purification. iTaq polymerase, 10X PCR buffer, and magnesium chloride were obtained from Bio-Rad (Montreal, QC Canada). Primers and dNTP mix (dATP, dCTP, dGTP and dTTP) were obtained from Sigma-Aldrich. Ethidium bromide (UltraPure 10 mg/mL, EtBr) was purchased from Life Technologies Inc. (Burlington, ON Canada). A 100 bp DNA ladder was purchased from BioLabs (Ipswich, MA).

2.2 Microchip fabrication

The microfluidic channels were laser-micromachined within X-PMMA substrates with a 10.6 µm CO_2 excimer laser engraving system (Universal Laser Systems, VLS2.30). The synthetic procedure for X-PMMA was adopted from Aly Saad Aly *et al*.[17] The channels were 2.5 cm in length, 500 µm wide, and 350 µm deep. To obtain an enclosed channel, another piece of the X-PMMA substrate with two holes drilled for the inlet and outlet was thermally bonded with the substrate hosting the microchannel, by placing the top and bottom substrates in a hot press under pressure (115 °C, 10^3 PSI) for 15 minutes (Heated Press 4386, Carver, Wabash, IN). To facilitate the tube connections between the microfluidic channel and the bacterial suspension reservoir, two 30G syringe needles were trimmed, set over the inlet and outlet of the microfluidic channel, and bonded with a mixture of epoxy glue and fumed silica powder to achieve a hard and stable adhesive layer.

2.3 Off-chip monolithic films

The compositions used to prepare the antibacterial networks, summarized in Table 1, were first investigated off-chip to study their antibacterial activity. To create a thin film of each composition on an X-PMMA substrate, each mixture was spin-coated on the substrate and then exposed to a UV source to initiate the polymerization. The substrates with the grafted film were then gently washed with methanol to remove any unreacted monomer and left to dry for 15 minutes in a fume hood.

Table 1: Composition of the monolith solutions used (in wt%).[a]

	Monomer	Cross-linker		
Monolith	DADMAC	EGDMA	1,6-HDDMA	EGDA
1	21	9	—	—
2	21	—	9	—
3	21	—	—	9

[a] All the reactions included 70% methanol as porogenic solvent and 0.2% DMPAP as photoinitiator.

2.4 PPM formation, characterization and stability

2.4.1 PPM formation

The mixtures of Table 1 were sonicated for 10 minutes to obtain homogeneous solutions, and were then introduced into the microchannel. Polymerization was triggered by irradiation of the substrate for 10 minutes with a 365 nm UV source in a cabinet containing a UV lamp (200 mJ/cm^2 intensity, ENF-260C, Spectronics Corp. Westbury, NY, USA). The substrate was then turned over and irradiated with the UV source on the other side for 10 minutes longer. Using a Pico plus syringe pump (Harvard apparatus, Holliston, MA), the microchannel was then flushed with methanol followed by deionized (DI) water to remove unreacted monomers and the porogenic solvent, respectively. As allyic monomers are sensitive to allylic chain transfer (Zimmerman 1961), DADMAC can potentially act as cross-linker. Thus we tried to photo-polymerize DADMAC with no cross-linker to form the PPM within the microfluidic channels, but the network was never formed. It is worth mentioning that the absorbance of the 20 % and 10 % X-PMMA samples at 365 nm was determined to be 0.238 and 0.101, respectively.

2.4.2 PPM characterization

Images for the monoliths were obtained with a Hitachi SU-70 scanning electron microscope (SEM, Hitachi High-Technologies Corporation, Tokyo, Japan) at an acceleration voltage of 10 kV. The SEM samples were prepared by immersing the microchannel hosting the PPM column into liquid nitrogen, and then cutting perpendicularly to the monolith-filled X-PMMA channel. To form an electrically conductive layer, gold was sputtered onto the samples prior to SEM imaging.

The pore size and porosity of the PPM columns were determined by mercury intrusion porosimetry using a Quantachrome Poremaster 60 device (Quantachrome Instruments, Boynton Beach, FL). The PPM columns were freeze-dried under vacuum and a sample of approximately 1 cm^3 was put into a sample holder cell to force mercury, a non-reactive and non-wetting liquid, into the pores of the sample. The relationship between the pressure applied and the diameter of the pores into which the mercury intruded was determined from the Washburn equation (Skudas et al. 2011).

2.4.3 Mechanical stability of PPM columns

Pressure tests were conducted to evaluate the mechanical stability of the monolithic columns within the microfluidic channel at different cross-linker contents in the PPM columns and the X-PMMA substrate. A pressure test was conducted to study the bonding strength by pumping ethanol pressurized by a compressed N_2 cylinder through it. The pressure was increased in 10 PSI increments every 5 minutes to determine the pressure at which the monolithic column started to debond from the substrate (PPM deponding pressure) and a leak started at the interface between the two substrate layers (Substrate deponding pressure).

2.5 Bacterial cultures

Pseudomonas putida and Escherichia coli were used as gram-negative test bacterial strains, while Micrococcus luteus (Schroeter) and Kocuria rosea were used as gram-positive strains. These bacterial strains were purchased from American Type Culture Collection (ATCC, Manassas, VA, catalog numbers: ATCC 12633, ATCC 35218, ATCC4698, and ATCC 186, respectively). Details about the bacterial cultures and the conditions of growth are provided as Supplementary Information.

2.6 Antibacterial, leaching and growth inhibition tests

The antibacterial activity of the cross-linked films, possible leaching from the PPM columns, and the ability of the PPM column materials to inhibit bacterial growth were studied as follows.

2.6.1 Antibacterial activity

The live/dead viability assay (L7012, Molecular Probe, Burlington, ON Canada) was used to investigate the interactions between the cross-linked films and bacterial cells. The assay used two fluorescent nucleic acid stains, SYTO 9 (green) and propidium iodide (PI; red). The two stains (0.15 µL of each) were mixed on a vortex mixer, 100 µL of bacterial suspension (Escherichia coli ATCC 35218) was added and mixed, and the stock mixture was incubated for 15 minutes at 37 ^{0}C. A 10 µL sample of bacterial suspension-stain mixture was dropped over the cross-linked film and covered with a thin microscope slide. The sandwiched layers were left in contact under the microscope, and images were recorded in the fluorescence mode after zero and 600 seconds of contact time.

The SYTO 9 stain penetrates both healthy bacterial cells (with intact membranes) and non-healthy cells; it therefore labels both live and dead bacteria. In contrast, propidium iodide penetrates only bacteria with damaged membranes, thus reducing the SYTO 9 fluorescence intensity. Consequently, live bacteria with intact membranes fluoresce green and dead bacteria (with disintegrated membranes) fluoresce red, while the background remains virtually non-fluorescent. Images were captured on a fluorescence microscope (Nikon Eclipse E600FN upright) with a digital camera (Nikon Photometrics Coolsnap EZ 12-Bit Monochrome Cooled CCD and NIS-ELEMENTS IMAGING Software) through a dual-band filter, so that both cells with and without intact cell membranes could be visualized simultaneously.

2.6.2 Leaching test

For each of the three PPM compositions of Table 1, two columns were synthesized within microfluidic channels. The microchannels were then flushed with methanol, followed by DI water, to remove unreacted monomers and porogenic solvents. To investigate subsequent leaching from each PPM column, PBS buffer was flown through for an hour in one case and for 24 hours in the other case. The PPM columns were then opened by cutting vertically through the monolith-filled X-PMMA channel with an electrical saw. The column material was removed by scraping and ground into a fine powder, mixed with KBr in a 1:30 weight ratio, and dried in a vacuum oven at 60 °C overnight. KBr pellets were prepared for analysis by pressing the powder in a dye at 10 kPSI for 3 minutes on a Carver 3851 Press (Thomas Scientific, Swedesboro, NJ). FT-IR spectra for each PPM column were acquired at room temperature on a Bruker Tensor 27 spectrometer, by averaging 64 scans recorded at a rate of 1 scan/sec. The wavenumber region scanned was between 400 and 4000 cm^{-1}.

To confirm leaching detected by FT-IR analysis, 100 µL of Escherichia coli bacterial suspension was pelletized at a relative centrifugal force (RCF) of 25500 (13000 RPM) for 3 minutes and re-suspended in 100 µL of the PBS buffer collected at the outlet of each PPM column after flowing through each column for 24 hours. It is noteworthy to mention that the PPM columns were first flushed with methanol, followed by DI water, to remove unreacted monomers and porogenic solvents before flowing the PBS buffer to ensure that there is no free monomer present before the leaching test. Using the serial dilution method each 100 µL sample was added, spread on solid agar dishes and incubated at 37 °C for 24 hours.

2.6.3 Bacterial growth inhibition

To investigate bacterial growth inhibition by the PPM networks, 4 mL of NB media, 10 µL of bacterial suspension (Micrococcus luteus (Schroeter) (ATCC 4698) or Pseudomonas putida (ATCC 12633)) and a 0.5 × 1 cm^2 slice of each of a film corresponding to the PPM columns compositions of Table 1 were placed in glass test tubes and incubated overnight in a shaker (200 RPM, 37 °C). The positive controls were two tubes containing 4 mL of NB media and 10 µL of gram-negative bacteria (Pseudomonas putida) in one tube, and 10 µL of gram-positive (Micrococcus luteus) bacteria in the other tube. The negative control was a tube containing 4 mL of NB media.

2.7 Cell Lysis efficiency

The bacterial cell lysate collected at the microchip outlet after flowing the bacterial suspension through each of the PPM columns described in Table 1, at a flow rate of 4 µL/min and cell concentrations as described in the Supplementary Information, was used to study the cell lysis efficiency of the PPM columns.

2.7.1 DNA detection by fluorometry

The ethidium bromide (EtBr) intercalation assay was used as an indicator of the presence of DNA in the cell lysate. A 20 µL aliquot of bacterial cell lysate was added to a spectrofluorometer cuvette containing 380 µL of DI water and 30 µL of EtBr from a stock solution with a concentration of 0.4 mg/L, and measured on a Quanta-Master 4 spectrofluorometer (Photon Technology International, London, ON Canada).

2.7.2 DNA concentration by UV-Vis spectrophotometry

A 4 µL aliquot of PBS buffer was pipetted onto the end of a fiber optic cable (the receiving fiber) of a UV-Vis Spectrophotometer NanoDrop 2000c (Thermo Scientific, Mississauga, ON) to use as a blank (reference). Another cable was brought into contact with the sample to connect the sample with the fiber optic ends. Then a 4 µL sample of Pseudomonas putida (ATCC 12633), Escherichia coli (ATCC 35218), Micrococcus luteus (Schroeter) (ATCC4698) or Kocuria rosea (ATCC 186) bacterial cell lysate was separately pipetted onto the receiving fiber to measure the DNA concentration in the lysate after flowing the cell suspension through each of the PPM columns.

To examine the reusability of the PPM columns, a single microchip was reused 40 times and the cell lysis efficiency was determined each time it was used. Escherichia coli bacteria were the species used in this test, in which they were suspended in PBS and was passed through the antibacterial monolith at a flow rate of 4 µL/min. The monolith was washed after each run with 25 µL of PBS buffer. To investigate the possibility of DNA carryover, the buffer used to flush the microfluidic channel was mixed with EtBr and the change in fluorescence intensity was recorded. Two control samples were used in these experiments: one containing 400 µL of DI water, and a second one containing 30 µL of EtBr (from a stock solution with a concentration of 0.4 mg/L), 380 µL of DI water, and 20 µL of PBS.

2.7.3 PCR reagents and experimental setup

The PCR reaction was performed in a T100 Thermal Cycler (Bio-RD, Montreal, QC Canada) in a 25 µL volume consisting of 300 nM of forward primer, 300 nM of reverse primer, 200 µM of dNTPs, 3.5 mM of magnesium chloride, 0.625 U of iTaq polymerase, 2.5 µL of 10X PCR buffer, and 200 ng of DNA present in the crude cell lysatecollected at the outlet of the microchip. More details about the structure of the primers and the PCR cycles details are provided as Supplementary Information (Table S1).

2.7.4 Gel electrophoresis

A Bio-Rad gel electrophoresis apparatus served to analyze the PCR products on 1.2% agarose gel using a DC voltage of 85 V and a running time of 30 minutes. The gel was subsequently removed from the chamber and was imaged with a Bio-Rad Doc XR imaging system.

3 Results and discussion

3.1 Monolith formation, characterization and stability

3.1.1 Monolith formation

It is noteworthy that none of the functional cross-linking monomer combinations of Table 1 could be dissolved in the commonly used porogenic solvent mixtures such as cyclohexanol and 1-dodecanol, thus several alternate solvents were investigated. Since it was reported that methanol could also serve as porogenic solvent to create porous networks (Yu et al. 2011; Yu et al. 2013), that solvent was used successfully for that purpose. It is also worth mentioning that several compositions (functional, cross-linker and solvent wt%) to form the PPM column were tried, but only with the composition listed in Table 1, a homogeneous mixture was formed and a cohesive stable structure was for the PPM column was polymerized within the microfluidic channel.

3.1.2 Monolith characterization

The SEM images obtained for the PPM columns with different cross-linking monomers are shown in Figure 1. For the images on the right, the microchips were incubated at 45 °C for 20 minutes prior to introducing the PPM mixture in the microfluidic channel and starting the polymerization. Looking at Figure 1, it can be noted that the poly(DADMAC-*co*-EDGA) PPM column is less porous than the poly(DADMAC-*co*-EGDMA) and poly(DADMAC-*co*-1,6-HDDMA) PPM columns. This result implies that the cross-linker structure affects the porosity of the PPM, in agreement with findings that were revealed in literature (Ranjha and Qureshi 2014). It can also be seen that the PPMs on the right are denser than the ones on the left. This effect is caused by pre-heating of the microchip prior to polymerization. The effect of temperature on the polymerization kinetics was previously investigated and it was found that it directly affects the morphology of the monolith surface, and as a result the porosity of the monolith (Nischang et al. 2009). Thus, the variations in PPM morphology and porosity seen in the SEM images on the right are in agreement with the results reported by Nischang *et al*.

The pore size and porosity of the PPM columns were determined by mercury intrusion porosimetry to clarify and confirm the SEM results. Porosimetry results for the three PPM columns are provided in Table 2. It can be seen that the porosimetry results are in agreement with the visual observations of the SEM images, thus confirming that the poly(DADMAC-co-EDGA) PPM column is less porous than the poly(DADMAC-co-EGDMA) and poly(DADMAC-co-1,6-HDDMA) PPM columns. Lower porosity may lead to more pronounced mechanical shearing of the cell membranes during flow through the pores of the PPM column.

Table 2: Pore size and porosity of the PPM columns was determined by mercury intrusion porosimetry.

PPM	Median pore diameter (µm)	Porosity (%)
DADMAC-*co*-EGDMA	5.5	75
DADMAC-*co*-1,6-HDDMA	4.8	71
DADMAC-*co*-EGDA	4	66

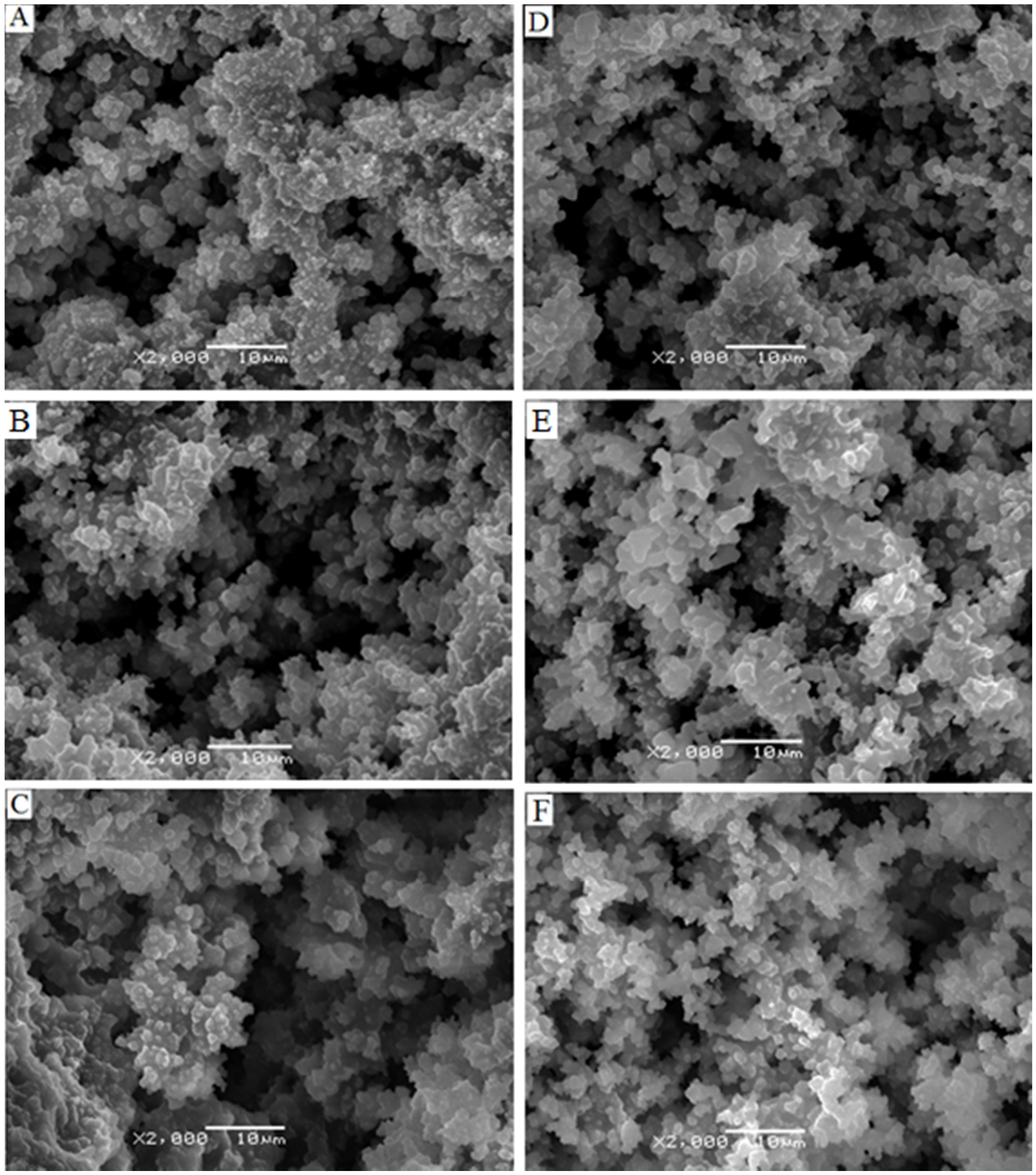

Figure 1: SEM images for the monolithic columns: (A), (B) and (C) are EGDMA, 1,6-HDDMA and EGDA-PPM, respectively; (D), (E) and (F) are the EGDMA, 1,6-HDDMA and EGDA-PPM formed in the pre-heated microchips, respectively.

3.1.2 Monolith stability

To confirm bonding between the PPM column and the X-PMMA substrate, and to quantify the bonding strength between the two substrate layers, pressure tests were conducted. The pressure withstood by the PPM column before it started to debond from the substrate and to move along the channel (as determined by visual inspection) is provided Figure 2 for the three PPM compositions studied in combination with X-PMMA substrates having 3, 5, 10, 15 and 20% cross-linker contents. From Figure 2 it can be seen that the three lines have positive slopes, which indicates that bonding or anchoring of the PPM column material to the substrate was improved as the cross-linking level of the substrate increased. Furthermore, the EGDA-cross-linked monolithic columns had stronger bonding to the substrate than the 1,6-HDDMA and EGDMA-cross-linked columns. The experiments performed to obtain Figure 2 were repeated three times and the results shown are the average of these results for each PPM. The standard deviation on the values obtained with each cross-linker (mole %) are displayed as error bars on Figure 2.

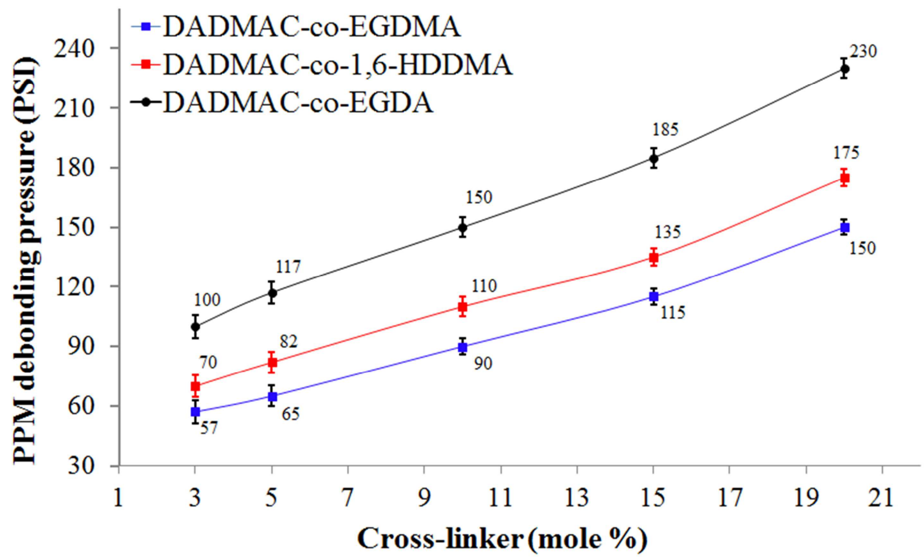

Figure 2: Debonding pressure of the monolithic column from the substrate for different X-PMMA cross-linking levels and different PPM compositions.

The substrate debonding pressure, at which the two substrate layers started to locally debond and a leak was observed at the interface, is provided in Figure 3. It can be seen that the curve has a negative slope, which indicates that bonding between the two substrate layers worsens as the cross-linking level increases. By comparing Figures 2 and 3, it can be concluded that EGD-cross-linked monolithic columns with the 10% X-PMMA substrate offers acceptable bonding between the PPM and the substrate and between the two substrate layers. The experiments performed to obtain Figure 3 were repeated three times and the results shown are the average of these results for each cross-linker (mole %). The standard deviation on the values obtained with each cross-linker (mole %) are displayed as error bars on Figure 3.

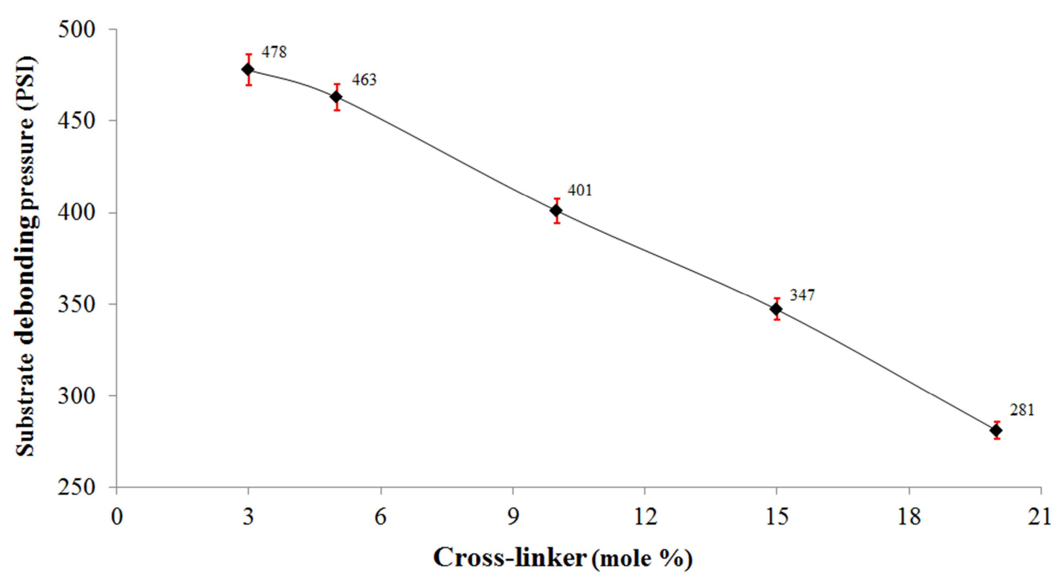

Figure 3: Debonding pressure of the two substrate layers at different X-PMMA cross-linking levels.

3.2 Antibacterial, leaching and growth inhibition tests

3.2.1 Antibacterial activity

Bacteria viability was monitored by the double staining technique described in Section 2.6.1. The green fluorescence was gradually replaced with red fluorescence in these experiments, as shown in Figure 4 A – D, providing clear evidence for membrane disintegration. It can be observed that the X-PMMA substrates grafted with the poly(DADMAC-*co*-EGDA) film led to more predominant red fluorescence than the substrates grafted with either poly(DADMAC-*co*-1,6-HDDMA) or poly(DADMAC-*co*-EGDMA) films, respectively. This implies that the poly(DADMAC-*co*-EGDA) film has a higher antibacterial activity than the poly(DADMAC-*co*-1,6-HDDMA) and poly(DADMAC-*co*-EGDMA) films.

The red and green fluorescence intensities were recorded for up to 600 seconds, as shown in Figure S3 of the the Supplementary Information. For the substrates grafted with the antibacterial films the green and red intensities decreased and increased with time, respectively, reflecting the fact that the cell membranes gradually became permeable, thus allowing propidium iodide to penetrate the cell membrane and reduce the fluorescence intensity from SYTO 9. This provides clear evidence that the substrates with the grafted cross-linked films are antibacterial. In contrast to the grafted substrates, the green and red fluorescence intensities for the control sample (pristine X-PMMA film) remained almost constant, reflecting the fact that no antibacterial activity is observed in that case. It can be also observed from Figure S3 that the rate of decrease and increase of the green and red fluorescence intensities for the three grafted substrates agree with the visual results of Figure 4.

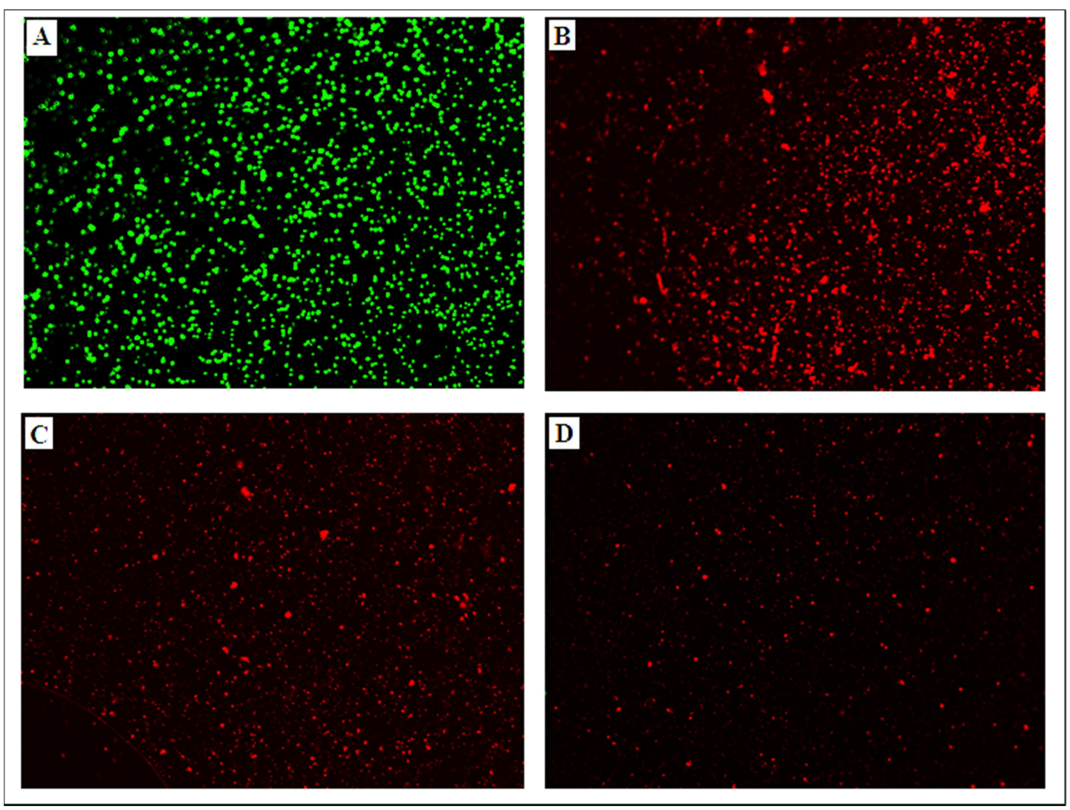

Figure 4: Fluorescence intensities for Escherichia coli suspended in PBS buffer and stained with live/dead dye in contact with (A) the three antibacterial networks at time zero, (B) poly(DADMAC-*co*-EGDA), (C) poly(DADMAC-*co*-1,6-HDDMA) and (D) poly(DADMAC-*co*-EGDMA) after 600 seconds.

3.2.2 Leaching tests

Leaching of DADMAC from the poly(DADMAC-*co*-EGDA), P(DADMAC-*co*-1,6-HDDMA) and P(DADMAC-*co*-EGDMA) monolithic columns was studied using FT-IR after flushing them with PBS buffer for either one hour or 24 hours. FT-IR spectra for the poly(DADMAC-*co*-EGDA) PPM column after 24 hours (Figure 5) shows that the peak for DADMAC in the cross-linked network was essentially unchanged in A and B, indicating that no significant leaching of DADMAC or poly(DADMAC) occurred. In contrast, the FT-IR peak absorption decreased for the poly(DADMAC-*co*-1,6 HDDMA) PPM column, while the effect was even more pronounced for the poly(DADMAC-*co*-EGDMA) PPM column.

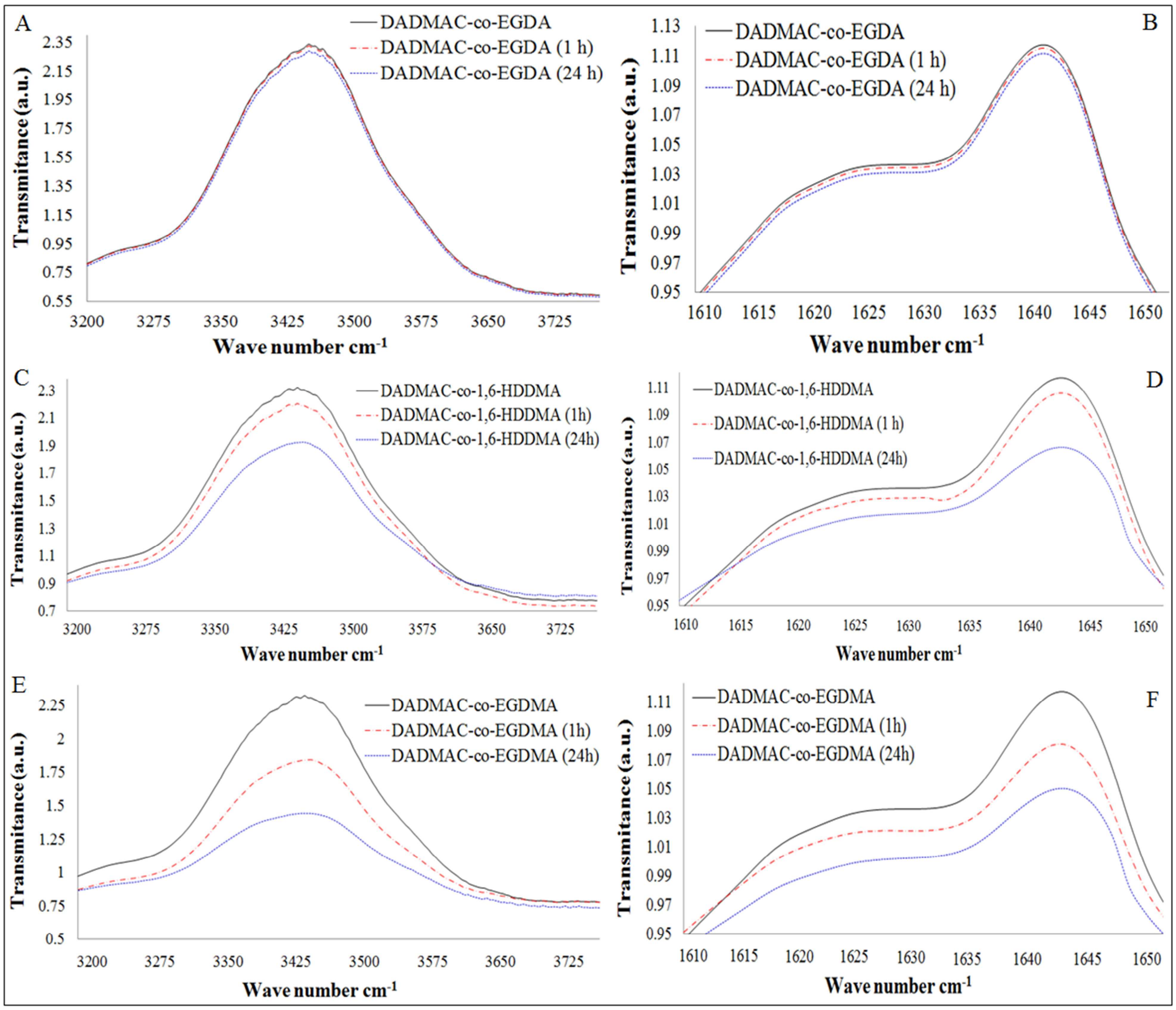

Figure 5: FT-IR spectra for the N–H stretching absorbance of the unsaturated primary amine groups (right) and C–N stretching vibration in the secondary amine group followed by NH bend (left) of (A, B) poly(DADMAC-*co*-EGDA), (C, D) poly(DADMAC-*co*-1,6-HDDMA), and (E, F) poly(DADMAC-*co*-EGDMA) before (black line), after 1 hour (red line) and after 24 hours (blue line) of washing with PBS.

To confirm the results obtained in the leaching test, Escherichia coli bacteria were re-suspended in the PBS buffer collected at the outlet of each PPM column in the 24 hours leaching test, applied onto solid agar dishes and then incubated at 37 °C. The colonies obtained on agar after 24 hours of incubation are shown in Figure 6. No colony was produced for the cells suspended in the PBS buffer collected in the leaching test for the poly(DADMAC-*co*-EGDMA) PPM column (as shown in Figure 6C), indicating that extensive leaching took place. In contrast, the plate for cells suspended in the PBS buffer collected in the leaching test for the poly(DMAMS-*co*-EGDA) PPM column has a large number of colonies on it, while the dish for the poly(DADMAC-*co*-1,6 HDDMA) PPM column has fewer colonies on it in comparison to the control dish. These results are in agreement with those obtained in the leaching tests. It is evident that the poly(DADMAC-*co*-EGDMA) PPM columns suffered from extensive leaching, while the poly(DADMAC-*co*-EGDA) PPM columns displayed very moderate leaching. The agar leaching experiment was repeated three times to confirm the results shown in Figure 6.

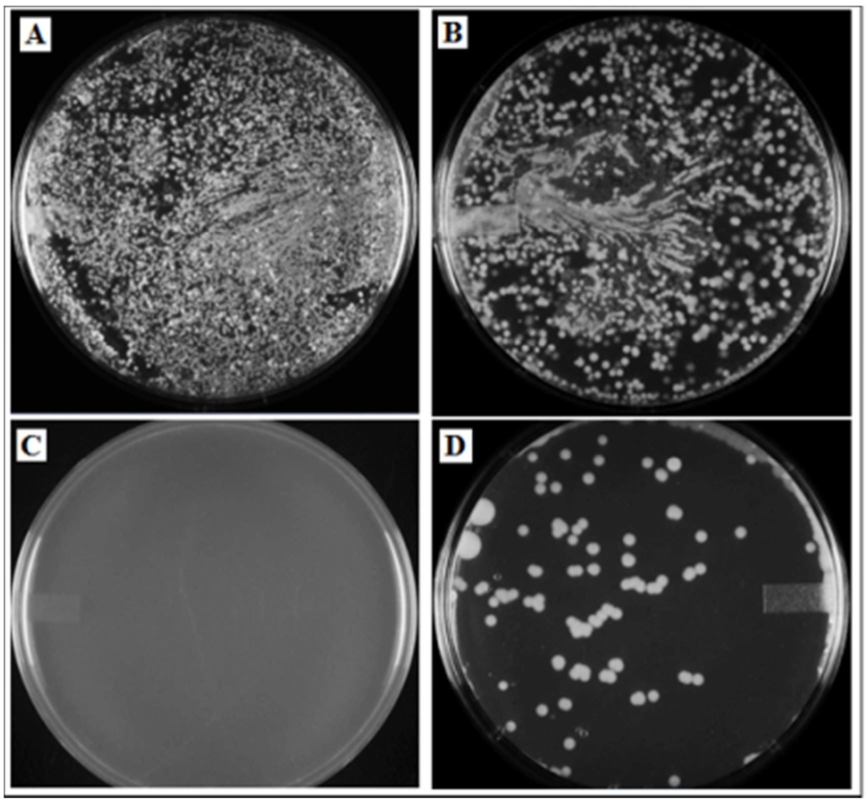

Figure 6: Colonies produced on agar after the 24 hours leaching tests for (A) control, (B) poly(DADMAC-*co*-EGDA), (C) poly(DADMAC-*co*-EGDMA), and (D) poly(DADMAC-*co*-1,6-HDDMA).

3.2.3 Growth inhibition test

The bacterial growth inhibition ability of the PPM column materials for gram-negative (P. putida) and gram-positive (M. luteus) bacteria is illustrated in Figure 7. The gram-negative and gram-positive control samples (Figure 7A and B, respectively) show healthy growth, with optical density values at 600 nm, OD_{600} = 2.38 and 2.012, respectively. In contrast, ATTC 12633 and ATCC 4698 bacterial samples with poly(DADMAC-*co*-EGDA), Figure 7C and D, poly(DADMAC-*co*-1,6-HDDMA), Figure 7E and F, or poly(DADMAC-*co*-EGDMA), Figure 7G and H, strips show major signs of growth inhibition with OD_{600} = 0.013, 0.019, 0.025, 0.030, 0.033, 0.039, respectively. These results validate the ability of the PPM column materials to inhibit gram-negative and gram-positive bacterial growth.

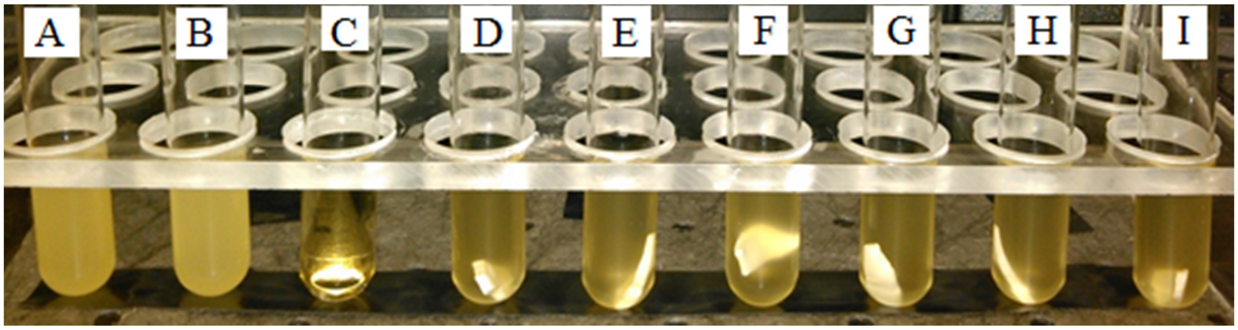

Figure 7: Bacterial growth inhibition for (A and B) positive controls (gram-negative, ATTC 12633 and gram-positive, ATCC 4698 bacteria overnight cultured in nutrient broth (NB) and trypticase soy broth (TSB), respectively), (C) negative control (NB media), (D and E), (F and G), and (H and I) gram-positive and gram-negative bacteria cultured overnight in TSB and NB media, respectively, with a 0.5 × 1 cm^2 strip of poly(DADMAC-*co*-EGDMA), poly(DADMAC-*co*-EGDA), and poly(DADMAC-*co*-1,6-HDDMA) monolith films, respectively.

3.4 Cell Lysis efficiency

3.4.1 DNA determination by fluorometry

To determine semi-quantitatively the DNA released after lysing the bacterial cells by flowing them through the antibacterial porous medium of the three PPM columns with the different compositions, the EtBr intercalation assay was used to detect DNA in the cell lysate. When EtBr is exposed to UV light at 285 nm it fluoresces with an orange color at 595 nm, but the emission intensifies considerably after its intercalation in DNA. The fluorescence intensity for EtBr before (control) and after intercalation in the DNA present in the cell lysate collected at the outlet of the porous antibacterial monoliths (1-3) was measured on a spectrofluorometer to obtain Figure 8. The figure clearly shows that the fluorescence intensity of EtBr increased when adding the cell lysate collected from the porous monolith columns, as compared to the control sample. It can be observed in Figure 8 that the fluorescence intensity for EtBr is higher for gram-negative bacteria (P. putida, E. coli) as compared to the gram-positive bacteria (M. luteus and K. rosea), which implies that more DNA is present in the gram-negative bacterial cell lysate. This is because gram-positive bacteria are harder to lyse than gram-negative bacteria, due to differences in the bacterial cell membrane structure for both bacterial species. The results also show that the fluorescence intensity of EtBr is slightly different among the four different gram-positive bacterial species, which could be due to size differences among the studied species. It can be further seen that the poly(DADMAC-*co*-EGDA) PPM has a higher lysis efficiency than the poly(DADMAC-*co*-1,6-HDDMA) and poly(DADMAC-*co*-EGDMA) PPMs. By recalling the results observed from Figure 1, Table 2, Figure 4 and Figure S3, showing that poly(DADMAC-*co*-EGDA) is less porous and has higher antibacterial activity than poly(DADMAC-*co*-1,6- HDDMA) and poly(DADMAC-*co*-EGDMA), this confirms that lysis was achieved by a combination of mechanical shearing and antibacterial activity resulting from interactions with the cell membrane, as reported previously by Aly Saad Aly *et al*.[17, 18] The experiments performed to obtain Figure 8 were repeated three times, and the results shown are the average of these experiments for each PPM. The standard deviations on the values obtained for each PPM are tabulated in Table S2 of the Supplementary Information.

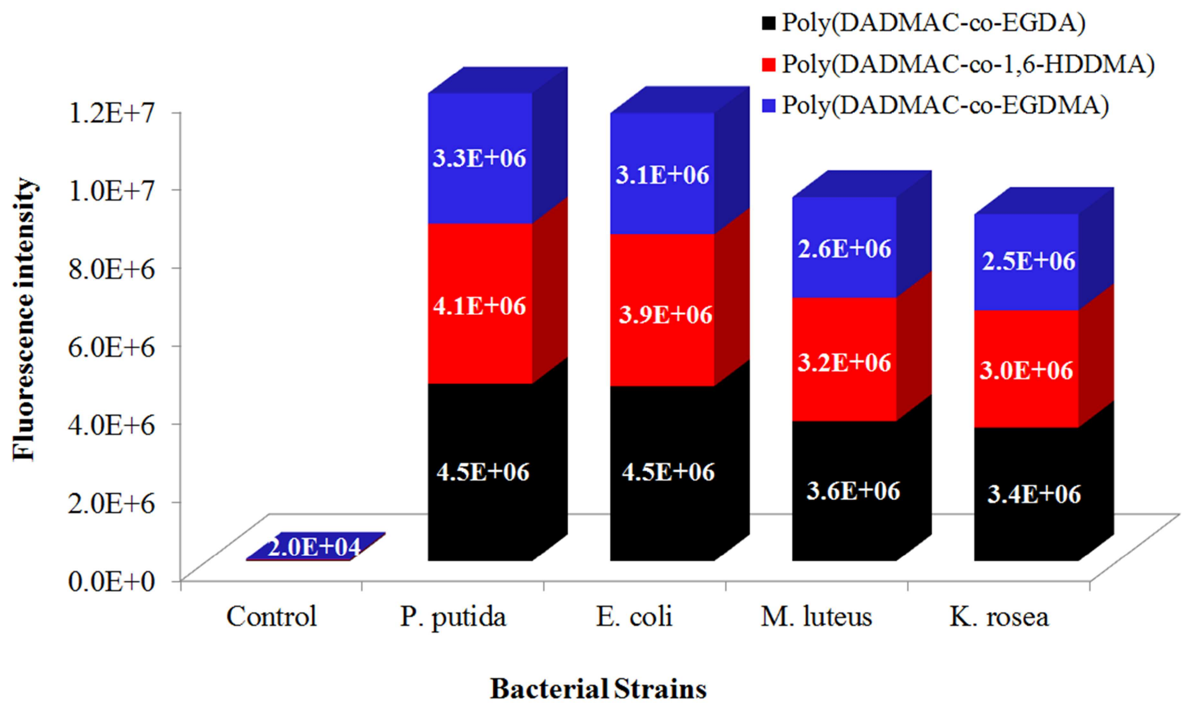

Figure 8: Fluorescence intensity for EtBr before (control) and after intercalating into DNA released after flowing the bacterial cells through the different PPM columns.

3.4.2 DNA concentration by UV-Vis spectrophotometry

To further validate cell lysis, the concentration of DNA released from the bacterial cells after flowing through the porous medium of the PPM columns was quantified by UV-Vis spectrophotometry as shown in Figure S4 of the Supplementary Information. It is evident from these results that the DNA concentration in the gram-negative (ATCC 12633 and ATCC 35218) bacterial cell lysates is greater than for the gram-positive (ATCC 4698 and ATCC 186) cell lysates. One can also note again that the DNA concentration varies slightly among the gram-negative bacterial cell lysates as well as among gram-negative cell lysates. The results also show that the poly(DADMAC-*co*-EGDA) PPM has a higher lysis efficiency than the poly(DADMAC-*co*-1,6-HDDMA) and poly(DADMAC-*co*-EGDMA) PPMs. The results presented in Figure S4 are in agreement with those shown in Figure 8. The experiments to obtain Figure S4 were repeated three times and the results shown are the average values obtained for each PPM. The corresponding standard deviations for each PPM are tabulated in Table S3 of the Supplementary Information.

3.4.3 PCR and gel electrophoresis

The genes in the DNA released by lysing the bacterial cells on the poly(DADMAC-*co*-EGDA) PPM column were amplified by off-chip PCR and qualitatively validated by gel electrophoresis. The analysis results are shown in Figure 9 for the PCR products of the different cell lines investigated. There are no detectable amounts of DNA at the PCR output for the bacteria samples that were not flown through the poly(DADMAC-*co*-EGDA) PPM column, which shows that the cells had intact membranes before passing through the PPM column. In contrast, DNA is clearly detected at the PCR output for the samples passed through the poly(DADMAC-*co*-EGDA) PPM column, which confirms that the membrane of the bacterial cells was disintegrated. This is not only a clear sign for lysis, but also demonstrates that the antibacterial PPM did not interfere with the PCR process.

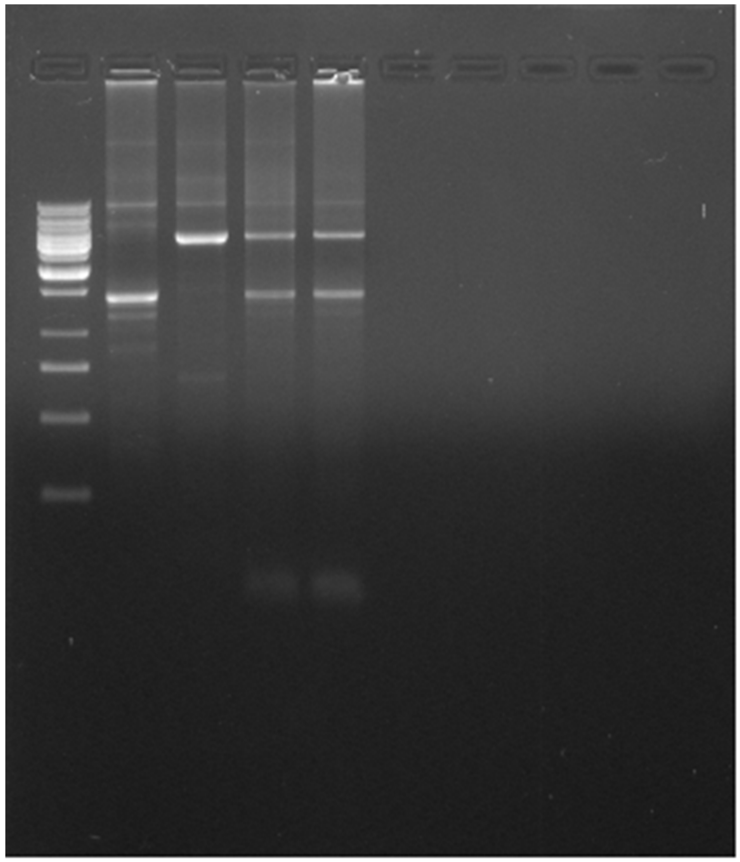

Figure 9: Gel electrophoresis analysis of PCR output. Column 1 (from the left) is for a 100 bp DNA ladder. Columns 2 and 6: lysed and unlysed ATCC 35218. Columns 3 and 7: lysed and unlysed ATCC 186. Columns 4 and 8: lysed and unlysed ATCC 12633. Columns 5 and 9: lysed and unlysed ATCC 4698.

3.5 Reusability of the microchips

The change in EtBr fluorescence due to the intercalation into the DNA in the cell lysate after each use of the microchip, when using a PBS wash between cycles, is shown in Figure 10. It can be seen that the lysis efficiency is reasonably stable, with a slight linear decrease over successive runs. After the thirtieth use, the lysis efficiency degrades dramatically however. It is worth mentioning that the monolith was completely blocked and degraded after 45 cycles. The microchip is therefore reusable, with acceptable degradation in lysis efficiency (9% decrease after 30 cycles). The florescence intensity measured for EtBr mixed with the PBS washings recovered from the microfluidic channel in the back-flush cycles showed insignificant DNA carryover, reaching only 0.4% of the maximum EtBr intensity reported, as shown in Table S4 of the Supplementary Information. It is interesting to note that the PPM column of Figure 10 can be reused for 10 more cycles than the optimized unprotected poly(*n*-butyl methacrylate-*co*-N-(*tert*-butyloxycarbonyl)aminoethyl methacrylate) (Boc-PPM) columns previously developed by Aly Saad Aly *et al.*,[18] and also with less DNA carryover. The antibacterial PPM columns presented in this work also do not require activation or regeneration by flowing phosphoric acid as in the previous case[18], thus leading to shorter lysis cycles when using QAC-PPM in comparison with the unprotected Boc-PPM columns.

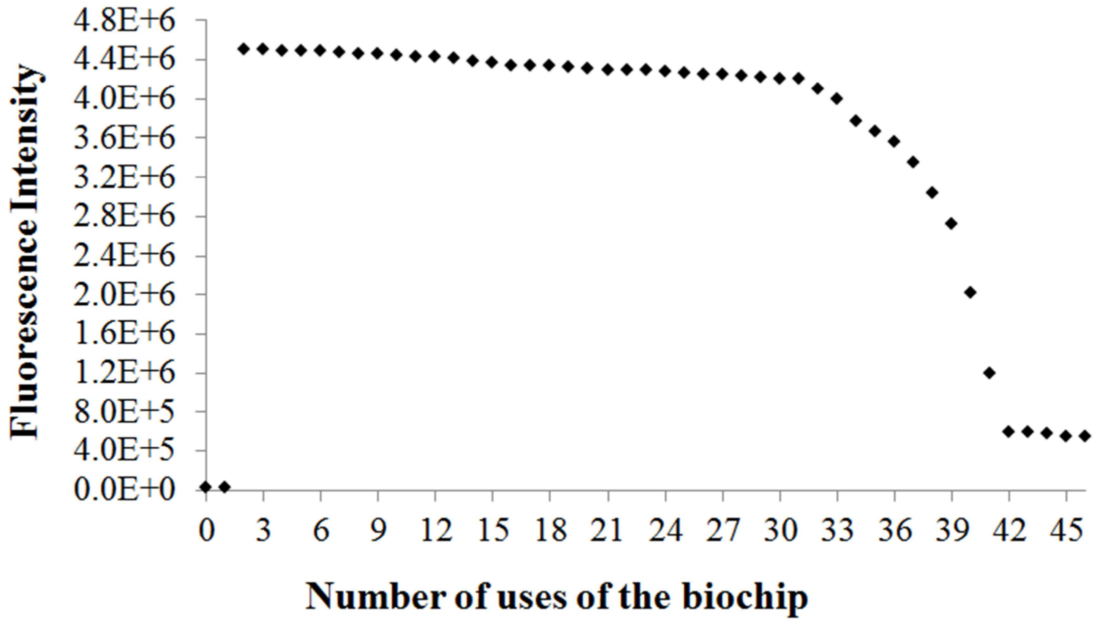

Figure 10: Fluorescence intensity for EtBr intercalated into the DNA released from bacterial cells flowing through the antibacterial poly(DADMAC-*co*-EGDA) monolith at a flow rate of 4 µL/min over successive runs.

4 Conclusions

Microfluidic biochips fabricated with a 10% X-PMMA substrate have the ability to inhibit the growth, kill, and efficiently lyse two species of gram-positive bacteria, M. luteus (ATCC 4698) and K. rosea (ATCC 186), and two species of gram-negative bacteria, P. putida (ATCC 12633) and E. coli (ATCC 35218). The lysis ability of the microchip was validated using the EtBr intercalation assay, by relating the presence of DNA in the cell lysate with an increase in fluorescence intensity for EtBr, and by UV-Vis spectrophotometry to directly determine the DNA concentration in the cell lysate. Gel electrophoresis analysis of the PCR products showed that the PPM columns do not leach any material that inhibits the PCR process. The influence of the cross-linking monomer on bacterial growth inhibition, leaching, the lysis efficiency of the monolithic column, and its mechanical stability within the microfluidic channel were investigated using three different cross-linking monomers: EGDA, EGDMA and 1,6-HDDMA at different cross-linking levels of the X-PMMA substrate. Furthermore, the bonding efficiency of the X-PMMA substrate layers at different cross-linking levels was studied. It was also shown that the microchips can be reused at least 30 times without significant performance degradation or carryover when they are flushed between cycles. It was concluded that the lysis time is shorter and that the number of reuse cycles increased for microchips based on the quaternary ammonium antibacterial PPM developed in this work in comparison to microfluidic biochips based on deprotected antibacterial poly(*n*-butyl methacrylate-*co*-N-(*tert*-butyloxycarbonyl)aminoethyl methacrylate) columns which we recently developed.[18]

References

M. Aly Saad Aly, O. Nguon, M. Gauthier and J. T. W. Yeow, RSC Adv. **3**, 24177 (2013)

M. Aly Saad Aly, M. Gauthier and J. T. W. Yeow, Anal. Bioanal. Chem. **406**, 5977 (2014)

A. Bhattacharyya, D. Kulinski and C. Klapperich, J. Vis. Exp. **12**, 664 (2008)

M. Biesalski and J. Ruhe, Macromolecules **32**, 2309 (1999)

L. Cen, K. G. Neoh and E. T. Kang, J. Biomed. Mater. Res. A. **71A**, 70 (2004)

B. Dizman, M. O. Elasri and L. J. Mathias, J. Polym. Sci. Pol. Chem. **44**, 5965 (2006)

M. Ignatova, S. Voccia, B. Gilbert, N. Markova, P. S. Mercuri, M. Galleni, V. Sciannamea, S. Lenoir, D. Cossement, G. Harkes, J. Dankert and J. Feijen, J. Biomat. Sci-Polym. E. **3**, 403 (1992)

E. Koslow, Structure that inhibit microbial growth, US Patent App. 11/832, 042 (2007).

S. B. Lee, R. R. Koepsel, S. W. Morley, K. Matyjaszewski, Y. Sun and A. J. Russell, Biomacromolecules **5**, 877 (2004)

K. Lienkamp, A. E. Madkour, A. Musante, C. T. Nelson, K. Nusslein and G. N. Tew, J. Am. Chem. Soc. **130**, 9836 (2008)

A. Lu, X. Wang and C. Xiao, Carbohyd. Polym. **37**, 427 (2008)

M. Mahalanabis, H. Al-Muayad, M. D. Kulinski, D. Altman and C. M. Kapperich, Lab Chip **9**, 2811 (2009)

A. Mikhaylova, B. Liesenfeld, D. Moore, W. Toreki, J. Vella, C. Batich and G. Schultz, Biotechnol. Bioeng. **23**, 24 (2011)

H. Murata, R. R. Koepsel, K. Matyjaszewski and A. J. Russell, Biomaterials **32**, 4870 (2007)

I. Nischang, T. Sevec and J. M. J. Frechet, Anal. Chem. **81**, 7390 (2009)

N. M. Ranjha and U. Qureshi, Int. J. Pharm. Pharm. Sci. **6**, 400 (2014)

A. F. Sauer-Budge and P. Mirer and A. Chatterjee and C. M. Klapperich and D. Chargin and A. Sharon, Lab Chip **9**, 2803 (2009)

R. Skudas, M. Thommes and K. U. Klaus, inCharacterization of the Pore Structure of Monolithic Silicas, ed.By K. K. Unger, N. Tanaka, E. Machtejevas (Wiley-VCH Verlag GmbH and Co., KGaA, Germany, 2011).

J. Thome, A. Hollander, W. Jaeger, I. Trick and C. Oehr, Surf. Coat. Tech. **174-175**, 584 (2003)

J. C. Tiller, C. Liao, K. Lewis and A. M. Klibanov, J. Am. chem. Soc. **98**, 5981 (2001)

R. Gouttebaron, R. Jerome and C. Jerome, Langmuir **20**, 10718 (2004)

H. C. van der Mei, M. Rustema-Abbing, D. E. Langworthy, D. I. Collias, M. D. Mitchell, D. W. Bjorkquist and H. J. Busscher, Biotechnol. Bioeng. **99**, 1097 (2008)

S. Yu, T. L. Ng, K. C. C. Ma, T. L. Ng, J. Zhao and S. K. K. Tong, J. Appl. Polym. Sci. **120**, 3190 (2011)

S. Yu, T. L. Ng, K. C. C. Ma, A. A. Mon, T. L. Ng and Y. Y. Ng, J. Appl. Polym. Sci. **127**, 2641 (2013)

J. Zimmerman, J. of Polym. Sci., 1961, 49, 247–252.